

---

# Can Decentralized Stochastic Minimax Optimization Algorithms Converge Linearly for Finite-Sum Nonconvex-Nonconcave Problems?

---

Yihan Zhang<sup>1</sup>

Wenhao Jiang<sup>2</sup>

Feng Zheng<sup>3</sup>

Chiu C. Tan<sup>1</sup>

Xinghua Shi<sup>1</sup>

Hongchang Gao<sup>1</sup>

<sup>1</sup>Temple University

<sup>2</sup>Tencent

<sup>3</sup>Southern University of Science and Technology

## Abstract

Decentralized minimax optimization has been actively studied in the past few years due to its application in a wide range of machine learning models. However, the current theoretical understanding of its convergence rate is far from satisfactory, since existing works only focus on the nonconvex-strongly-concave problem. This motivates us to study decentralized minimax optimization algorithms for the nonconvex-nonconcave problem. To this end, we develop two novel decentralized stochastic variance-reduced gradient descent ascent algorithms for the finite-sum nonconvex-nonconcave problem that satisfies the Polyak-Łojasiewicz (PL) condition. In particular, our theoretical analyses demonstrate how to conduct local update and perform communication to achieve the linear convergence rate. To the best of our knowledge, this is the first work achieving linear convergence rates for decentralized nonconvex-nonconcave problems. Finally, we verify the performance of our algorithms on both synthetic and real-world datasets. The experimental results confirm the efficacy of our algorithms.

## 1 INTRODUCTION

A wide range of machine learning models can be formulated as a minimax optimization problem, such as adversarially robust machine learning models Goodfellow et al. [2014a,b], Madry et al. [2017], distributionally robust machine learning models Lin et al. [2020], Luo et al. [2020], AUC maximization models Ying et al. [2016], Liu et al. [2019], just name a few. To facilitate such kinds of machine learning models for distributed data, this paper studies the decentralized

finite-sum minimax problem, which is defined as follows:

$$\min_{x \in \mathbb{R}^{d_x}} \max_{y \in \mathbb{R}^{d_y}} f(x, y) \triangleq \frac{1}{K} \sum_{k=1}^K \left( \frac{1}{n} \sum_{i=1}^n f_i^{(k)}(x, y) \right), \quad (1)$$

where  $k \in \{1, 2, \dots, K\}$  is the index of worker,  $f^{(k)}(x, y) \triangleq \frac{1}{n} \sum_{i=1}^n f_i^{(k)}(x, y)$  denotes the loss function on the  $k$ -th worker,  $f_i^{(k)}(x, y)$  represents the loss function of the  $i$ -th sample on the  $k$ -th worker. Here, all workers compose a communication graph and its adjacency matrix is denoted by  $W = [w_{ij}] \in \mathbb{R}_+^{K \times K}$ , where  $w_{ij} > 0$  denotes worker  $i$  and  $j$  are connected, otherwise  $w_{ij} = 0$ . Based on such a communication graph, the worker conducts peer-to-peer communication.

In this paper, we consider the decentralized nonconvex-nonconcave minimax problem that satisfies the PL condition, which is still unexplored and more challenging than the nonconvex-strongly-concave minimax problem. In fact, such a condition is satisfied in many applications, such as overparameterized neural networks Liu et al. [2022], robust phase retrieval model Sun et al. [2018], deep AUC maximization model Liu et al. [2019], just name a few. Until very recently, the convergence of minimax optimization algorithms under the PL condition has been studied by Yang et al. [2020], Chen et al. [2022a] under the single-machine setting. In particular, Yang et al. [2020] investigated the alternating gradient descent ascent (AGDA) algorithm, which demonstrated that the variance-reduced variant enjoys the linear convergence rate. Chen et al. [2022a] shows that the variance-reduced stochastic gradient descent ascent (SGDA) algorithms can also achieve the linear convergence rate even though they do not take the alternating update rule.

Obviously, the aforementioned minimax optimization algorithms show promising performance under the single-machine setting. Then, a natural question arises: *Can decentralized stochastic minimax optimization algorithms converge linearly for nonconvex-nonconcave problems that satisfy the PL condition?*

In fact, the decentralized setting brings unique challenges to investigate the convergence behavior. Specifically, each worker under the decentralized setting updates its local model parameters with its own gradient. Additionally, due to the decentralized communication strategy, there does not exist global communication. This results in large consensus errors between local model parameters and global model parameters, which has an adverse effect on the convergence rate. Currently, it is unclear whether the consensus error will make the linear convergence rate unachievable. Then, it is necessary to study how the consensus error affects the convergence rate and design new algorithms to alleviate the large consensus error issue.

## 1.1 CONTRIBUTIONS

To address the aforementioned questions, we develop two decentralized stochastic variance-reduced gradient descent ascent (DSVRGDA) algorithms for the finite-sum minimax optimization problem that satisfies the PL condition. Generally speaking, our study discovered that the traditional decentralized communication strategy cannot make DSVRGDA achieve the linear convergence rate due to the large consensus error. Therefore, to mitigate the large consensus error, we compensate the traditional decentralized communication strategy with the stage-wise multi-round communication. As such, the consensus error can be reset to zero stage-wisely and then our algorithms are able to achieve the linear convergence rate. In summary, we made the following contributions in this paper.

- We develop two decentralized stochastic variance-reduced gradient descent ascent algorithms based on the gradient-tracking communication strategy and stage-wise multi-round communication strategy. As far as we know, this is the first time showing how to conduct local update and perform communication for the aforementioned minimax problem.
- We establish the convergence rate of our two decentralized algorithms for the finite-sum minimax optimization problem that satisfies the PL condition. They both can achieve the linear convergence rate. To the best of our knowledge, this is the first work achieving linear convergence rate for such a kind of decentralized minimax problem.
- We evaluate our two algorithms on both synthetic and real-world datasets. The extensive experimental results confirm the effectiveness of our two algorithms.

## 2 RELATED WORKS

In this section, we briefly introduce the convergence rate of existing minimax optimization and decentralized optimization problems.

### 2.1 MINIMAX OPTIMIZATION

Since many emerging machine learning models, e.g., adversarial generative networks Goodfellow et al. [2014b], can be formulated as a minimax optimization problem, how to efficiently optimize this kind of problem has been extensively studied in recent years. In particular, under the single-machine setting, Lin et al. [2020] established the convergence rate of stochastic gradient descent ascent (SGDA) for nonconvex-strongly-concave problems, i.e.,  $O(1/\epsilon^4)$  to achieve the  $\epsilon$ -accuracy solution. Luo et al. [2020] improved it to  $O(n + n^{1/2}/\epsilon^2)$  for finite-sum problems with the SPIDER Fang et al. [2018], Nguyen et al. [2017] gradient estimator. Huang et al. [2020] leveraged the STORM Cutkosky and Orabona [2019] gradient estimator to improve the convergence rate to  $O(1/\epsilon^4)$  for stochastic problems.

When the objective function satisfies the PL condition, Yang et al. [2020] investigated the convergence rate of the alternating gradient descent ascent (AGDA) algorithm, i.e., two variables should be updated sequentially. In particular, Yang et al. [2020] showed that AGDA can achieve the linear convergence rate when using full gradient, but it fails to achieve that when employing stochastic gradient. Then, Yang et al. [2020] exploits the variance-reduced gradient estimator Johnson and Zhang [2013] to make the algorithm achieve linear convergence rate. Recently, Chen et al. [2022a] studied the convergence rate of SGDA for the minimax optimization problem that satisfies PL conditions. In particular, Chen et al. [2022a] developed two variance-reduced SGDA algorithms based on Johnson and Zhang [2013] and Fang et al. [2018], Nguyen et al. [2017] respectively, which demonstrated a linear convergence rate for finite-sum problems. All aforementioned algorithms only concentrate on the single-machine setting so that they cannot be utilized to optimize Eq. (1).

### 2.2 DECENTRALIZED OPTIMIZATION

Decentralized optimization has been widely leveraged to train machine learning models for distributed data. Currently, numerous algorithms have been proposed for the minimization problem. For example, Lian et al. [2017] developed the decentralized stochastic gradient descent (DSGD) algorithm based on the gossip communication strategy and demonstrated that the communication topology only affects the high-order term of the convergence rate for nonconvex problems. Lu et al. [2019] proposed a DSGD algorithm based on the gradient-tracking communication scheme. After that, Sun et al. [2020], Xin et al. [2020] improved the convergence rate of DSGD with variance-reduced gradient estimators Fang et al. [2018], Nguyen et al. [2017], Cutkosky and Orabona [2019] for finite-sum and stochastic problems. Since these algorithms are designed for minimization problem, they cannot be used to optimize Eq. (1).

As for decentralized minimax optimization, Xian et al. [2021] proposed a decentralized stochastic gradient descent ascent with the STORM Cutkosky and Orabona [2019] gradient estimator algorithm and established its convergence rate for stochastic nonconvex-strongly-concave problems. Zhang et al. [2021] employed the SPIDER Fang et al. [2018], Nguyen et al. [2017] gradient estimator for decentralized SGDA and provided its convergence rate for finite-sum problems. Later, Gao [2022] resorted to the ZeroSARAH Li and Richtárik [2021] gradient estimator and then improved the convergence rate of Zhang et al. [2021]. More recently, Chen et al. [2022b] further improved the communication complexity of Zhang et al. [2021], Gao [2022] with a multi-step communication strategy, but suffers from a worse sample complexity than Gao [2022]. All these theoretical convergence results only hold for nonconvex-strongly-concave problems. It is still unclear how decentralized minimax optimization algorithms converge under the PL condition.

### 3 PRELIMINARIES

In this section, we provide some fundamental definitions and assumptions for studying the convergence rate of our algorithms.

**Definition 1.** A function  $f(x) : \mathbb{R}^d \rightarrow \mathbb{R}$  satisfies the  $\mu$ -PL (Polyak-Łojasiewicz) condition if there exists  $\mu > 0$  such that

$$2\mu(f(x) - f(x_*)) \leq \|\nabla f(x)\|^2, \quad \forall x \in \mathbb{R}^d, \quad (2)$$

where  $x_* = \arg \min_{x' \in \mathbb{R}^d} f(x')$ .

It is worth noting that the PL condition is weaker than strong convexity. A strongly convex function satisfies the PL condition, but not vice versa. For instance, a nonconvex function, e.g., the overparameterized neural network Liu et al. [2022], can also satisfy the PL condition.

Based on this definition, we introduce the following assumptions for the loss function in Eq. (1).

**Assumption 1.** The function  $f(\cdot, \tilde{y})$  satisfies the  $\mu$ -PL condition for any fixed  $\tilde{y} \in \mathbb{R}^{d_y}$ , i.e., for  $\forall x \in \mathbb{R}^{d_x}$ , there exists  $\mu > 0$  such that

$$2\mu(f(x, \tilde{y}) - \min_{x' \in \mathbb{R}^{d_x}} f(x', \tilde{y})) \leq \|\nabla_x f(x, \tilde{y})\|^2. \quad (3)$$

Similarly,  $-f(\tilde{x}, \cdot)$  satisfies the  $\mu$ -PL condition for any fixed  $\tilde{x} \in \mathbb{R}^{d_x}$ , i.e., for  $\forall y \in \mathbb{R}^{d_y}$ , there exists  $\mu > 0$  such that

$$2\mu(-f(\tilde{x}, y) + \max_{y' \in \mathbb{R}^{d_y}} f(\tilde{x}, y')) \leq \|\nabla_y f(\tilde{x}, y)\|^2. \quad (4)$$

**Assumption 2.** For  $\forall k \in \{1, 2, \dots, K\}$  and  $\forall i \in \{1, 2, \dots, n\}$ ,  $f_i^{(k)}(\cdot, \cdot)$  is  $L$ -smooth, i.e.,

$$\begin{aligned} & \|\nabla f_i^{(k)}(x_1, y_1) - \nabla f_i^{(k)}(x_2, y_2)\|^2 \\ & \leq L^2 \|x_1 - x_2\|^2 + L^2 \|y_1 - y_2\|^2, \end{aligned} \quad (5)$$

where  $L > 0$  is a constant value,

Based on Assumption 1-2, we denote the condition number as  $\kappa = L/\mu$ .

Under the decentralized setting, we have the following assumptions for the adjacency matrix, which are commonly used in existing decentralized optimization literature Xian et al. [2021], Zhang et al. [2021], Gao [2022]

**Assumption 3.** 1)  $W$  is doubly stochastic and symmetric. 2) Its eigenvalues satisfy  $|\lambda_K| \leq |\lambda_{K-1}| \leq \dots \leq |\lambda_2| < |\lambda_1| = 1$ .

Based on Assumption 3, we denote  $\lambda = |\lambda_2|$  so that the spectral gap can be represented as  $1 - \lambda$ . Moreover, we denote the diameter of the communication graph as  $D$ .

Under these assumptions, the goal of this work is to find the  $\epsilon$ -saddle point of Eq. (1), i.e., a solution  $x$  satisfies  $g(x) - g(x^*) \leq \epsilon$  where  $g(x) \triangleq \max_{y \in \mathbb{R}^{d_y}} f(x, y)$ . Here, we assume the saddle point does exist. In particular, we have the following assumption.

**Assumption 4.** Yang et al. [2020], Chen et al. [2022a] The function  $f(x, y)$  has at least one saddle point  $(x^*, y^*)$ . Moreover, for any fixed  $\tilde{y} \in \mathbb{R}^{d_y}$ , the solution set of the subproblem  $\min_{x \in \mathbb{R}^{d_x}} f(x, \tilde{y})$  is not empty and its optimal value is finite. This is also true for the subproblem  $\min_{y \in \mathbb{R}^{d_y}} f(\tilde{x}, y)$  when fixing  $\tilde{x} \in \mathbb{R}^{d_x}$ .

Furthermore, from Lemma A.5 in Nouiehed et al. [2019], we can know that  $g(x)$  is  $L_g$ -smooth where  $L_g = 2L^2/\mu$ .

## 4 DECENTRALIZED MINIMAX OPTIMIZATION ALGORITHMS

In this section, we present the detail of our decentralized optimization algorithms to show how to do local update and perform communication.

### 4.1 DSVRGDA-P

In Algorithm 1, we proposed a novel decentralized stochastic variance-reduced gradient descent ascent algorithm DSVRGDA-P based on the PAGE gradient estimator Li et al. [2021]. Generally speaking, this is a stage-wise algorithm. In detail, in each stage  $s$ , each worker  $k$  is initialized with the same model parameters, i.e.,  $x_{s,0}^{(k)} = \tilde{x}_s^{(k)}$ ,  $y_{s,0}^{(k)} = \tilde{y}_s^{(k)}$ . In fact, this step is critical to achieve linear convergence rate, which will be discussed in details in the next section. Then, in each inner iteration  $r$ , each worker  $k$  computes the gradient estimator for the variable  $x$  as follows:

$$\phi_{s,r}^{(k)} = \begin{cases} \nabla_x f^{(k)}(x_{s,r}, y_{s,r}^{(k)}), & \text{with probability } p \\ \phi_{s,r-1}^{(k)} + \Delta_{s,r}^{(k)}(x), & \text{with probability } 1 - p \end{cases}, \quad (6)$$

---

**Algorithm 1** DSVRGDA-P
 

---

**Input:**  $\tilde{x}_0^{(k)} = x_0, \tilde{y}_0^{(k)} = y_0, \eta_x > 0, \eta_y > 0$ .

- 1: **for**  $s = 0, \dots, S - 1$ , each worker  $k$  **do**
- 2:  $x_{s,0}^{(k)} = \tilde{x}_s^{(k)}, y_{s,0}^{(k)} = \tilde{y}_s^{(k)}$ ,
- 3: **for**  $r = 0, \dots, R - 1$ , each worker  $k$  **do**
- 4: **if**  $r == 0$  **then**
- 5:  $\phi_{s,r}^{(k)} = \nabla_x f^{(k)}(x_{s,r}^{(k)}, y_{s,r}^{(k)})$ ,  
 $\psi_{s,r}^{(k)} = \nabla_y f^{(k)}(x_{s,r}^{(k)}, y_{s,r}^{(k)})$ ,
- 6: **else**
- 7: Compute the gradient estimator  $\phi_{s,r}^{(k)}$  and  $\psi_{s,r}^{(k)}$   
as Eq. (6) and Eq. (7),
- 8: **end if**
- 9: **if**  $r == 0$  **then**
- 10:  $u_{s,r}^{(k)} = \phi_{s,r}^{(k)}, v_{s,r}^{(k)} = \psi_{s,r}^{(k)}$ ,
- 11: **else**
- 12:  $u_{s,r}^{(k)} = \sum_{j \in \mathcal{N}_k} w_{kj} u_{s,r-1}^{(k)} - \phi_{s,r-1}^{(k)} + \phi_{s,r}^{(k)}$ ,  
 $v_{s,r}^{(k)} = \sum_{j \in \mathcal{N}_k} w_{kj} v_{s,r-1}^{(k)} - \psi_{s,r-1}^{(k)} + \psi_{s,r}^{(k)}$ ,
- 13: **end if**
- 14:  $x_{s,r+1}^{(k)} = \sum_{j \in \mathcal{N}_k} w_{kj} x_{s,r}^{(j)} - \eta_x u_{s,r}^{(k)}$ ,  
 $y_{s,r+1}^{(k)} = \sum_{j \in \mathcal{N}_k} w_{kj} y_{s,r}^{(j)} + \eta_y v_{s,r}^{(k)}$ ,
- 15: **end for**
- 16: Randomly choose  $(\tilde{x}_{s+1}^{(k)}, \tilde{y}_{s+1}^{(k)})$  from  
 $\{(\tilde{x}_{s,r}^{(k)}, \tilde{y}_{s,r}^{(k)})\}_{r=0}^{R-1}$  with the same random seed  
for all workers,
- 17: Conduct  $D$ -round communication such that  
 $\tilde{x}_{s+1}^{(k)} = \frac{1}{K} \sum_{k'=1}^K \tilde{x}_{s+1}^{(k')}, \tilde{y}_{s+1}^{(k)} = \frac{1}{K} \sum_{k'=1}^K \tilde{y}_{s+1}^{(k')}$ ,
- 18: **end for**

---

where  $\Delta_{s,r}^{(k)}(x) = \frac{1}{b} \sum_{i \in \mathcal{B}_{s,r}^{(k)}} (\nabla_x f_i^{(k)}(x_{s,r}^{(k)}, y_{s,r}^{(k)}) - \nabla_x f_i^{(k)}(x_{s,r-1}^{(k)}, y_{s,r-1}^{(k)}))$ ,  $\mathcal{B}_{s,r}^{(k)}$  is the randomly selected mini-batch with the batch size  $b$ . Similarly, each worker  $k$  computes the gradient estimator for the variable  $y$  as follows:

$$\psi_{s,r}^{(k)} = \begin{cases} \nabla_y f^{(k)}(x_{s,r}^{(k)}, y_{s,r}^{(k)}), & \text{with probability } p \\ \psi_{s,r-1}^{(k)} + \Delta_{s,r}^{(k)}(y), & \text{with probability } 1 - p \end{cases}, \quad (7)$$

where  $\Delta_{s,r}^{(k)}(y) = \frac{1}{b} \sum_{i \in \mathcal{B}_{s,r}^{(k)}} (\nabla_y f_i^{(k)}(x_{s,r}^{(k)}, y_{s,r}^{(k)}) - \nabla_y f_i^{(k)}(x_{s,r-1}^{(k)}, y_{s,r-1}^{(k)}))$ .

After that, each worker  $k$  leverages the gradient-tracking communication strategy to compute  $u_{s,r}^{(k)}$  and  $v_{s,r}^{(k)}$  as shown in Step 12 of Algorithm 1, where  $\mathcal{N}_k$  includes the neighboring workers of the  $k$ -th worker and itself. Then, based on these gradients, each worker  $k$  updates its local model parameters  $x_{s,r+1}^{(k)}$  and  $y_{s,r+1}^{(k)}$  as shown in Step 14 of Algorithm 1, where  $\eta_x > 0$  and  $\eta_y > 0$  are the learning rate.

After finishing the inner loop, each worker  $k$  randomly selects a solution from  $\{(\tilde{x}_{s,r}^{(k)}, \tilde{y}_{s,r}^{(k)})\}_{r=0}^{R-1}$  with the same random seed as  $(\tilde{x}_{s+1}^{(k)}, \tilde{y}_{s+1}^{(k)})$ . Then, in Step 17, DSVRGDA-P conducts multi-round communication to obtain the global variable. In fact, it can be done in  $D$  round for a graph

whose diameter is  $D$  Vogels et al. [2021]. For instance, it can be done in  $D = K - 1$  communication round for a line graph Scaman et al. [2017]. *This stage-wisely multi-round communication strategy is critical to achieve the linear convergence rate, which will be demonstrated in next section.*

To the best of our knowledge, this is the first work proposing this kind of communication strategy to guarantee the linear convergence rate. Thus, our algorithmic design is novel.

---

**Algorithm 2** DSVRGDA-Z
 

---

**Input:**  $\tilde{x}_0^{(k)} = x_0, \tilde{y}_0^{(k)} = y_0, \eta_x > 0, \eta_y > 0$ .

- 1: **for**  $s = 0, \dots, S - 1$ , each worker  $k$  **do**
- 2:  $x_{s,0}^{(k)} = \tilde{x}_s^{(k)}, y_{s,0}^{(k)} = \tilde{y}_s^{(k)}$ ,  
 $g_{s,-1}^{(k)}(i) = 0, h_{s,-1}^{(k)}(i) = 0$  for  $i \in \{1, 2, \dots, n\}$ ,
- 3: **for**  $r = 0, \dots, R - 1$ , each worker  $k$  **do**
- 4: **if**  $r == 0$  **then**
- 5:  $\phi_{s,r}^{(k)} = \frac{1}{b_0} \sum_{i \in \mathcal{B}_{s,0}} \nabla_x f_i^{(k)}(x_{s,r}^{(k)}, y_{s,r}^{(k)})$ ,  
 $\psi_{s,r}^{(k)} = \frac{1}{b_0} \sum_{i \in \mathcal{B}_{s,0}} \nabla_y f_i^{(k)}(x_{s,r}^{(k)}, y_{s,r}^{(k)})$ ,
- 6: **else**
- 7: Compute the gradient estimator  $\phi_{s,r}^{(k)}$  and  $\psi_{s,r}^{(k)}$   
as Eq. (8) and Eq. (9),
- 8: **end if**
- 9: **if**  $r == 0$  **then**
- 10:  $u_{s,r}^{(k)} = \phi_{s,r}^{(k)}, v_{s,r}^{(k)} = \psi_{s,r}^{(k)}$ ,
- 11: **else**
- 12:  $u_{s,r}^{(k)} = \sum_{j \in \mathcal{N}_k} w_{kj} u_{s,r-1}^{(k)} - \phi_{s,r-1}^{(k)} + \phi_{s,r}^{(k)}$ ,  
 $v_{s,r}^{(k)} = \sum_{j \in \mathcal{N}_k} w_{kj} v_{s,r-1}^{(k)} - \psi_{s,r-1}^{(k)} + \psi_{s,r}^{(k)}$ ,
- 13: **end if**
- 14:  $x_{s,r+1}^{(k)} = \sum_{j \in \mathcal{N}_k} w_{kj} x_{s,r}^{(j)} - \eta_x u_{s,r}^{(k)}$ ,  
 $y_{s,r+1}^{(k)} = \sum_{j \in \mathcal{N}_k} w_{kj} y_{s,r}^{(j)} + \eta_y v_{s,r}^{(k)}$ ,
- 15: Update  $g$  and  $h$ :  
 $g_{s,r}^{(k)}(i) = \begin{cases} \nabla_x f_i^{(k)}(x_{s,r}^{(k)}, y_{s,r}^{(k)}), & \text{for } i \in \mathcal{B}_{s,r}^{(k)} \\ g_{s,r-1}^{(k)}(i), & \text{otherwise} \end{cases}$   
 $h_{s,r}^{(k)}(i) = \begin{cases} \nabla_y f_i^{(k)}(x_{s,r}^{(k)}, y_{s,r}^{(k)}), & \text{for } i \in \mathcal{B}_{s,r}^{(k)} \\ h_{s,r-1}^{(k)}(i), & \text{otherwise} \end{cases}$
- 16: **end for**
- 17: Randomly choose  $(\tilde{x}_{s+1}^{(k)}, \tilde{y}_{s+1}^{(k)})$  from  
 $\{(\tilde{x}_{s,r}^{(k)}, \tilde{y}_{s,r}^{(k)})\}_{r=0}^{R-1}$  with the same random seed  
for all workers,
- 18: Conduct  $D$ -round communication such that  
 $\tilde{x}_{s+1}^{(k)} = \frac{1}{K} \sum_{k'=1}^K \tilde{x}_{s+1}^{(k')}, \tilde{y}_{s+1}^{(k)} = \frac{1}{K} \sum_{k'=1}^K \tilde{y}_{s+1}^{(k')}$ ,
- 19: **end for**

---

**4.2 DSVRGDA-Z**

From Eq. (6) and Eq. (7), it can be observed that the full gradient should be computed with the probability  $p$ . Then, to avoid the computation of the full gradient, we propose a novel stochastic variance-reduced gradient descent ascent algorithm DSVRGDA-Z based on the ZeroSARAH gradient estimator Li and Richtárik [2021], which is shown in

Algorithm 2. In detail, each worker  $k$  computes the gradient estimator  $\phi_{s,r}^{(k)}$  as follows:

$$\begin{aligned} \phi_{s,r}^{(k)} &= (1 - \rho)\phi_{s,r-1}^{(k)} + \rho \left( \frac{1}{n} \sum_{j=1}^n g_{s,r-1}^{(k)}(j) \right. \\ &+ \frac{1}{b_1} \sum_{i \in \mathcal{B}_{s,r}^{(k)}} (\nabla_x f_i^{(k)}(x_{s,r-1}^{(k)}, y_{s,r-1}^{(k)}) - g_{s,r-1}^{(k)}(i)) \\ &+ \left. \frac{1}{b_1} \sum_{i \in \mathcal{B}_{s,r}^{(k)}} (\nabla_x f_i^{(k)}(x_{s,r}^{(k)}, y_{s,r}^{(k)}) - \nabla_x f_i^{(k)}(x_{s,r-1}^{(k)}, y_{s,r-1}^{(k)})) \right), \end{aligned} \quad (8)$$

where  $\rho > 0$  is a constant value,  $b_1 = |\mathcal{B}_{s,r}^{(k)}|$ ,  $g_{s,r-1}^{(k)}(i)$  stores the stochastic gradient of the  $i$ -th sample, which is updated as shown in Step 19 of Algorithm 2. Obviously, when  $\rho = 0$ , this gradient estimator degenerates to SPIDER. An advantage of  $\phi_{s,r}^{(k)}$  is that we don't need to compute the full gradient so that it is more efficient than Algorithm 1, especially for a deep neural network where computing gradients through backpropagation is time-consuming. Similarly, each worker  $k$  computes the gradient estimator  $\psi_{s,r}^{(k)}$  as follows:

$$\begin{aligned} \psi_{s,r}^{(k)} &= (1 - \rho)\psi_{s,r-1}^{(k)} + \rho \left( \frac{1}{n} \sum_{j=1}^n h_{s,r-1}^{(k)}(j) \right. \\ &+ \frac{1}{b_1} \sum_{i \in \mathcal{B}_{s,r}^{(k)}} (\nabla_y f_i^{(k)}(x_{s,r-1}^{(k)}, y_{s,r-1}^{(k)}) - h_{s,r-1}^{(k)}(i)) \\ &+ \left. \frac{1}{b_1} \sum_{i \in \mathcal{B}_{s,r}^{(k)}} (\nabla_y f_i^{(k)}(x_{s,r}^{(k)}, y_{s,r}^{(k)}) - \nabla_y f_i^{(k)}(x_{s,r-1}^{(k)}, y_{s,r-1}^{(k)})) \right), \end{aligned} \quad (9)$$

where  $h_{s,r-1}^{(k)}(i)$  stores the stochastic gradient of the  $i$ -th sample and updated in Step 15 of Algorithm 2. The communication and local update for gradients and model parameters are the same with Algorithm 1.

In summary, we develop two novel decentralized optimization algorithms for optimizing Eq. (1). With this novel design regarding local update and stage-wise communication, our algorithms are able to achieve the linear convergence rate when the objective function satisfies the PL condition, which will be shown in next section.

## 5 CONVERGENCE RATE

In this section, we present the convergence rate of our two algorithms, especially showing why the stage-wise global communication is necessary.

To investigate the theoretical convergence rate of our algorithms, we employ the following metric, which is also used in existing works Chen et al. [2022a], Yang et al. [2020].

$$\mathcal{M}_s \triangleq \mathbb{E}[g(\bar{x}_s) - g(x_*)] + \frac{c_0 \eta_x}{\eta_y} \mathbb{E}[g(\bar{x}_s) - f(\bar{x}_s, \bar{y}_s)], \quad (10)$$

where  $c_0 = \frac{16L^2}{\mu^2}$ ,  $\bar{x}_s = \frac{1}{K} \sum_{k=1}^K \tilde{x}_s^{(k)}$ ,  $\bar{y}_s = \frac{1}{K} \sum_{k=1}^K \tilde{y}_s^{(k)}$ .

### 5.1 CONVERGENCE RATE OF ALGORITHM 1

To establish the convergence rate of Algorithm 1, we propose a novel potential function, which is defined as follows:

$$\begin{aligned} \mathcal{P}_{s,r} &= \mathbb{E}[g(\bar{x}_{s,r}) - g(x_*)] + \frac{c_0 \eta_x}{\eta_y} \mathbb{E}[g(\bar{x}_{s,r}) - f(\bar{x}_{s,r}, \bar{y}_{s,r})] \\ &+ c_1 \frac{1}{K} \mathbb{E}[\|X_{s,r} - \bar{X}_{s,r}\|_F^2] + c_2 \frac{1}{K} \mathbb{E}[\|Y_{s,r} - \bar{Y}_{s,r}\|_F^2] \\ &+ c_3 \frac{1}{K} \mathbb{E}[\|U_{s,r} - \bar{U}_{s,r}\|_F^2] + c_4 \frac{1}{K} \mathbb{E}[\|V_{s,r} - \bar{V}_{s,r}\|_F^2] \\ &+ c_5 \frac{1}{K} \sum_{k=1}^K \mathbb{E}[\|\phi^{(k)}(x_{s,r}^{(k)}, y_{s,r}^{(k)}) - \nabla_x f^{(k)}(x_{s,r}^{(k)}, y_{s,r}^{(k)})\|^2] \\ &+ c_6 \frac{1}{K} \sum_{k=1}^K \mathbb{E}[\|\psi^{(k)}(x_{s,r}^{(k)}, y_{s,r}^{(k)}) - \nabla_y f^{(k)}(x_{s,r}^{(k)}, y_{s,r}^{(k)})\|^2], \end{aligned} \quad (11)$$

where  $c_1 = \frac{80c_0 \eta_x L^2}{1-\lambda} \left(1 + \frac{(1-p)}{pb}\right)$ ,  $c_2 = \frac{80c_0 \eta_x L^2}{1-\lambda} \left(1 + \frac{(1-p)}{pb}\right)$ ,  $c_3 = (1-\lambda)\eta_x$ ,  $c_4 = (1-\lambda)c_0\eta_x$ ,  $c_5 = \frac{5\eta_x}{p}$ ,  $c_6 = \frac{5c_0\eta_x}{p}$ .

**Proposition 1.** *Given Assumptions 1-3, by setting  $\eta_x = \frac{\eta_y}{10c_0}$ ,  $\eta_x \leq \min\{\eta_{x,1}, \eta_{x,2}, \frac{1}{L_g}\}$ ,  $\eta_y \leq \min\{\eta_{y,1}, \eta_{y,2}, \frac{1}{L}\}$ , where*

$$\begin{aligned} \eta_{x,1} &= \frac{(1-\lambda)^2 \mu}{44L^2 \sqrt{1 + (1-p)/(pb)}}, \\ \eta_{x,2} &= \frac{\mu}{L^2} \frac{-6 + \sqrt{36 + 12800(1 + (1-p)/(pb))}}{12800(1 + (1-p)/(pb))}, \\ \eta_{y,1} &= \frac{(1-\lambda)^2}{11L \sqrt{1 + (1-p)/(pb)}}, \\ \eta_{y,2} &= \frac{1 - \frac{1}{2} + \sqrt{\frac{1}{4} + 80(1 + (1-p)/(pb))}}{L \sqrt{80(1 + (1-p)/(pb))}}, \end{aligned} \quad (12)$$

Algorithm 1 satisfies

$$\begin{aligned} &\mathbb{E}[g(\bar{x}_{s+1}) - g(x_*)] + \frac{c_0 \eta_x}{\eta_y} \mathbb{E}[g(\bar{x}_{s+1}) - f(\bar{x}_{s+1}, \bar{y}_{s+1})] \\ &\leq \frac{2}{\eta_x \mu R} \left( \mathbb{E}[g(\bar{x}_s) - g(x_*)] + \frac{c_0 \eta_x}{\eta_y} \mathbb{E}[g(\bar{x}_s) - f(\bar{x}_s, \bar{y}_s)] \right) \\ &\quad + \frac{2}{\eta_x \mu R} \hat{\mathcal{P}}_{s,0}, \end{aligned} \quad (13)$$

where  $\hat{\mathcal{P}}_{s,0}$  denotes the last six terms of  $\mathcal{P}_{s,0}$ .

**Remark 1.** *In terms of Proposition 1, to achieve the linear convergence rate,  $\hat{\mathcal{P}}_{s,0}$  should be zero. In terms of Algorithm 1, the full gradient is computed in the first iteration so that the last four terms of the potential function  $\hat{\mathcal{P}}_{s,0}$  are zero values. Then, we can use the multi-round communication to let  $\mathbb{E}[\|X_{s,0} - \bar{X}_{s,0}\|_F^2] = 0$  and  $\mathbb{E}[\|Y_{s,0} - \bar{Y}_{s,0}\|_F^2] = 0$  to make Algorithm 1 achieve the linear convergence rate.*

That is the reason why we should use the multi-round communication stage-wisely. Otherwise, the consensus errors  $\mathbb{E}[\|X_{s,0} - \bar{X}_{s,0}\|_F^2]$  and  $\mathbb{E}[\|Y_{s,0} - \bar{Y}_{s,0}\|_F^2]$  prevents Algorithm 1 from achieving linear convergence rate.

**Theorem 1.** Given Assumptions 1-3, by setting  $\eta_x = O(\frac{(1-\lambda)^2}{\kappa^2 L \sqrt{1+(1-p)/(pb)}})$ ,  $\eta_y = O(\frac{(1-\lambda)^2}{L \sqrt{1+(1-p)/(pb)}})$ ,  $R = \frac{4}{\eta_x \mu}$ , Algorithm 1 satisfies

$$\mathcal{M}_{s+1} \leq \frac{1}{2} \mathcal{M}_s, \quad (14)$$

which implies the linear convergence rate.

**Corollary 1.** In terms of Theorem 1, to find the solution such that  $\mathbb{E}[g(\bar{x}_s) - g(x_*)] \leq \epsilon$  and  $\mathbb{E}[g(\bar{x}_s) - f(\bar{x}_s, \bar{y}_s)] \leq 10\epsilon$ , by setting  $b = \sqrt{n}$  and  $p = \frac{b}{n+b}$ , we can get  $\eta_x = O(\frac{(1-\lambda)^2}{\kappa^2 L})$ ,  $\eta_y = O(\frac{(1-\lambda)^2}{L})$ ,  $R = O(\frac{\kappa^3}{(1-\lambda)^2})$ , the iteration complexity is  $O(\frac{\kappa^3}{(1-\lambda)^2} \log \frac{1}{\epsilon})$ , the sample complexity is  $O((n + \frac{\sqrt{n}\kappa^3}{(1-\lambda)^2}) \log \frac{1}{\epsilon})$ , and the communication complexity is  $O((D + \frac{\kappa^3}{(1-\lambda)^2}) \log \frac{1}{\epsilon})$ .

**Remark 2.** When the communication graph is fully connected, i.e.,  $1 - \lambda = 1$ , our sample complexity can match the state-of-the-art algorithm SPIDER-GDA Chen et al. [2022a] under the single-machine setting.

To the best of our knowledge, this is the first decentralized optimization algorithm that can achieve the linear convergence rate for nonconvex-nonconcave optimization problems satisfying PL conditions.

## 5.2 CONVERGENCE RATE OF ALGORITHM 2

To establish the convergence rate of Algorithm 2, we introduce the following potential function:

$$\begin{aligned} \mathcal{P}_{s,r} = & \mathbb{E}[g(\bar{x}_{s,r}) - g(x_*)] + \frac{c_0 \eta_x}{\eta_y} \mathbb{E}[g(\bar{x}_{s,r}) - f(\bar{x}_{s,r}, \bar{y}_{s,r})] \\ & + c_1 \frac{1}{K} \mathbb{E}[\|X_{s,r} - \bar{X}_{s,r}\|_F^2] + c_2 \frac{1}{K} \mathbb{E}[\|Y_{s,r} - \bar{Y}_{s,r}\|_F^2] \\ & + c_3 \frac{1}{K} \mathbb{E}[\|U_{s,r} - \bar{U}_{s,r}\|_F^2] + c_4 \frac{1}{K} \mathbb{E}[\|V_{s,r} - \bar{V}_{s,r}\|_F^2] \\ & + c_5 \frac{1}{K} \sum_{k=1}^K \mathbb{E}[\|\phi^{(k)}(x_{s,r}^{(k)}, y_{s,r}^{(k)}) - \nabla_x f^{(k)}(x_{s,r}^{(k)}, y_{s,r}^{(k)})\|^2] \\ & + c_6 \frac{1}{K} \sum_{k=1}^K \mathbb{E}[\|\psi^{(k)}(x_{s,r}^{(k)}, y_{s,r}^{(k)}) - \nabla_y f^{(k)}(x_{s,r}^{(k)}, y_{s,r}^{(k)})\|^2] \\ & + c_7 \frac{1}{K} \sum_{k=1}^K \mathbb{E}[\frac{1}{n} \sum_{j=1}^n \|\nabla_x f_j^{(k)}(x_{s,r}^{(k)}, y_{s,r}^{(k)}) - g_{s,r}^{(k)}(j)\|^2] \\ & + c_8 \frac{1}{K} \sum_{k=1}^K \mathbb{E}[\frac{1}{n} \sum_{j=1}^n \|\nabla_y f_j^{(k)}(x_{s,r}^{(k)}, y_{s,r}^{(k)}) - h_{s,r}^{(k)}(j)\|^2], \end{aligned} \quad (15)$$

where  $c_1 = c_2 = \frac{c_0 \eta_x L^2}{(1-\lambda)} \left(52 + \frac{160}{\rho b_1} + \frac{1920 \rho n^2}{b_1^3}\right)$ ,  $c_3 = (1-\lambda)\eta_x$ ,  $c_4 = (1-\lambda)c_0 \eta_x$ ,  $c_5 = \frac{5\eta_x}{\rho}$ ,  $c_6 = \frac{5c_0 \eta_x}{\rho}$ ,  $c_7 = \frac{30n\rho\eta_x}{b_1^2}$ ,  $c_8 = \frac{30n\rho c_0 \eta_x}{b_1^2}$ . Then, we can obtain the following proposition.

**Proposition 2.** Given Assumptions 1-3, by setting  $\eta_x = \frac{\eta_y}{10c_0}$ ,  $\eta_x \leq \min\{\eta_{x,1}, \eta_{x,2}, \frac{1}{L_g}\}$ ,  $\eta_y \leq \min\{\eta_{y,1}, \eta_{y,2}, \frac{1}{L}\}$ , where

$$\begin{aligned} \eta_{x,1} &= \frac{(1-\lambda)^2 \mu}{4L^2 \sqrt{76 + 240/(\rho b_1) + 1880\rho n^2/b_1^3}}, \\ \eta_{x,2} &= \frac{\mu}{L^2} \frac{-6 + \sqrt{36 + 80(6 + 20/(\rho b_1) + 240\rho n^2/b_1^3)}}{1280(6 + 20/(\rho b_1) + 240\rho n^2/b_1^3)}, \\ \eta_{y,1} &= \frac{(1-\lambda)^2}{L \sqrt{76 + 240/(\rho b_1) + 1880\rho n^2/b_1^3}}, \\ \eta_{y,2} &= \frac{1}{L} \frac{-1/2 + \sqrt{1/4 + 8(6 + 20/(\rho b_1) + 240\rho n^2/b_1^3)}}{8(6 + 20/(\rho b_1) + 240\rho n^2/b_1^3)}, \end{aligned} \quad (16)$$

Algorithm 2 satisfies

$$\begin{aligned} & \mathbb{E}[g(\bar{x}_{s+1}) - g(x_*)] + \frac{c_0 \eta_x}{\eta_y} \mathbb{E}[g(\bar{x}_{s+1}) - f(\bar{x}_{s+1}, \bar{y}_{s+1})] \\ & \leq \frac{2}{\eta_x \mu R} \left( \mathbb{E}[g(\bar{x}_s) - g(x_*)] + \frac{c_0 \eta_x}{\eta_y} \mathbb{E}[g(\bar{x}_s) - f(\bar{x}_s, \bar{y}_s)] \right) \\ & \quad + O\left(\frac{2}{\mu R}\right) \frac{1}{K} \left( \mathbb{E}[\|X_{s,0} - \bar{X}_{s,0}\|_F^2] + \mathbb{E}[\|Y_{s,0} - \bar{Y}_{s,0}\|_F^2] \right) \\ & \quad + O\left(\frac{c_0}{\mu R}\right) \frac{n - b_0}{(n-1)b_0} \frac{1}{K} \sum_{k=1}^K \frac{1}{n} \sum_{i=1}^n \mathbb{E}[\|\nabla_x f_i^{(k)}(x_{s,0}^{(k)}, y_{s,0}^{(k)})\|^2] \\ & \quad + O\left(\frac{c_0}{\mu R}\right) \frac{n - b_0}{(n-1)b_0} \frac{1}{K} \sum_{k=1}^K \frac{1}{n} \sum_{i=1}^n \mathbb{E}[\|\nabla_y f_i^{(k)}(x_{s,0}^{(k)}, y_{s,0}^{(k)})\|^2] \\ & \quad + O\left(\frac{2c_0}{\mu R}\right) \left(1 - \frac{b_0}{n}\right) \frac{1}{K} \sum_{k=1}^K \frac{1}{n} \sum_{j=1}^n \mathbb{E}[\|\nabla_x f_j^{(k)}(x_{s,0}^{(k)}, y_{s,0}^{(k)})\|^2] \\ & \quad + O\left(\frac{2c_0}{\mu R}\right) \left(1 - \frac{b_0}{n}\right) \frac{1}{K} \sum_{k=1}^K \frac{1}{n} \sum_{j=1}^n \mathbb{E}[\|\nabla_y f_j^{(k)}(x_{s,0}^{(k)}, y_{s,0}^{(k)})\|^2]. \end{aligned} \quad (17)$$

Similarly, we can get the linear convergence rate for Algorithm 2 as follows.

**Theorem 2.** Given Assumptions 1-3, by setting  $b_0 = n$ ,  $b_1 = \sqrt{n}$ ,  $\rho = \frac{b_1}{2n}$ ,  $\eta_x = O(\frac{(1-\lambda)^2}{\kappa^2 L})$ ,  $\eta_y = O(\frac{(1-\lambda)^2}{L})$ ,  $R = \frac{4}{\eta_x \mu}$ , Algorithm 2 satisfies

$$\mathcal{M}_{s+1} \leq \frac{1}{2} \mathcal{M}_s, \quad (18)$$

which implies the linear convergence rate.

**Corollary 2.** In terms of Theorem 2, to find the solution such that  $\mathbb{E}[g(\bar{x}_s) - g(x_*)] \leq \epsilon$  and  $\mathbb{E}[g(\bar{x}_s) - f(\bar{x}_s, \bar{y}_s)] \leq 10\epsilon$ , by setting the hyperparameters as shown in Theorem 2,

the iteration complexity of Algorithm 2 is  $O(\frac{\kappa^3}{(1-\lambda)^2} \log \frac{1}{\epsilon})$ , the sample complexity is  $O((n + \frac{\sqrt{n}\kappa^3}{(1-\lambda)^2}) \log \frac{1}{\epsilon})$ , and the communication complexity is  $O((D + \frac{\kappa^3}{(1-\lambda)^2}) \log \frac{1}{\epsilon})$ .

## 6 EXPERIMENT

In this section, we conduct extensive experiments to verify the performance of our algorithms.

### 6.1 EXPERIMENTAL SETUP

**Synthetic Data.** To verify the performance of our algorithms, we first focus on the following two player Polyak-Lojasiewicz game:

$$\min_{x \in \mathbb{R}^{10}} \max_{y \in \mathbb{R}^{10}} \frac{1}{K} \sum_{k=1}^K \left( \frac{1}{2} x^T A^{(k)} x - \frac{1}{2} y^T B^{(k)} y + x^T C^{(k)} y \right), \quad (19)$$

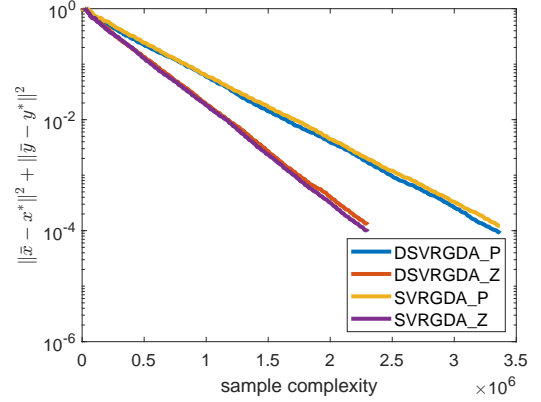
where  $A^{(k)} = \frac{1}{n} \sum_{i=1}^n a_i^{(k)} (a_i^{(k)})^T$ ,  $B^{(k)} = \frac{1}{n} \sum_{i=1}^n b_i^{(k)} (b_i^{(k)})^T$ , and  $C^{(k)} = \frac{1}{n} \sum_{i=1}^n c_i^{(k)} (c_i^{(k)})^T$ . Following Chen et al. [2022a],  $a_i^{(k)}$ ,  $b_i^{(k)}$ , and  $c_i^{(k)}$  are independently drawn from Gaussian distributions  $\mathcal{G}(0, \Sigma_{A^{(k)}})$ ,  $\mathcal{G}(0, \Sigma_{B^{(k)}})$ , and  $\mathcal{G}(0, \Sigma_{C^{(k)}})$ , respectively. Here, the covariance matrices  $\Sigma_{A^{(k)}}$  and  $\Sigma_{B^{(k)}}$  are constructed via  $P\Lambda P^T$ <sup>1</sup>, where  $P \in \mathbb{R}^{10 \times 5}$  has orthogonal columns and  $\Lambda \in \mathbb{R}^{5 \times 5}$  is a diagonal matrix. Additionally, the diagonal elements of  $\Lambda$  are uniformly drawn from  $[10^{-5}, 1]$ . As for  $\Sigma_{C^{(k)}}$ , it is constructed via  $0.1QQ^T$ , where  $Q \in \mathbb{R}^{10 \times 10}$  and the elements of  $P$  are drawn from Gaussian distribution  $\mathcal{G}(0, 1)$ . In this way, the objective function satisfies the PL condition, but not strongly-convex-strongly-concave condition Karimi et al. [2016], Chen et al. [2022a]. In our experiment, we set  $n = 600$ .

**Real-world Data.** We also verify the performance of our algorithms on real-world data. Specifically, we focus on the AUC maximization problem for the binary classification task, which is formulated as the following minimax optimization problem:

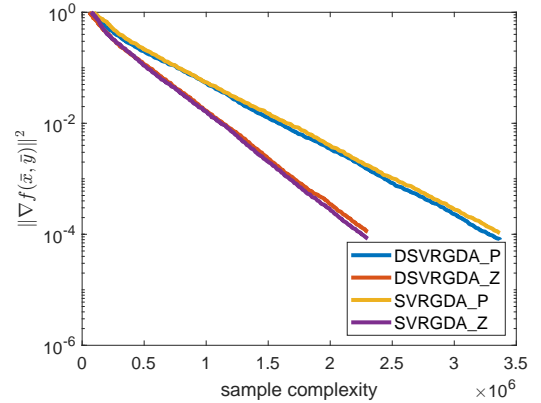
$$\begin{aligned} \min_{x, \hat{x}_1, \hat{x}_2} \max_y \frac{1}{K} \sum_{k=1}^K \frac{1}{n} \sum_{i=1}^n & \left( (1-p)(x^T a_i^{(k)} - \hat{x}_1)^2 \mathbb{I}_{[b_i^{(k)}=1]} \right. \\ & + 2(1+y)(px^T a_i^{(k)} \mathbb{I}_{[b_i^{(k)}=-1]} - (1-p)x^T a_i^{(k)} \mathbb{I}_{[b_i^{(k)}=1]}) \\ & \left. + p(x^T a_i^{(k)} - \hat{x}_2)^2 \mathbb{I}_{[b_i^{(k)}=-1]} - p(1-p)y^2 + \gamma \mathcal{R}(x) \right), \end{aligned} \quad (20)$$

where  $x \in \mathbb{R}^d$  is the classifier's parameter,  $\hat{x}_1 \in \mathbb{R}$ ,  $\hat{x}_2 \in \mathbb{R}$ ,  $y \in \mathbb{R}$  are the parameters to compute the AUC loss,  $(a_i^{(k)}, b_i^{(k)})$  is the  $i$ -th sample's feature and label on the  $k$ -th worker,  $p$  is the prior probability of positive class,  $\mathbb{I}$  is

an indicator function,  $\mathcal{R}(x) = \sum_{j=1}^d \frac{x_j^2}{1+x_j^2}$  is the regularization term,  $\gamma > 0$  denotes the hyperparameter. For this task, we employ three benchmark datasets: a9a, w8a, and ijcnn1, which can be found from LIBSVM Data website<sup>2</sup>. In our experiments, we randomly select 20% of samples as the testing set and use the other samples as the training set.



(a) Distance to saddle point



(b) Norm of gradient

Figure 1: The comparison between different algorithms for Eq. (19). Line graph is used.

**Experimental Settings.** Since our algorithms are the first one for the minimax problem satisfying PL conditions, there does not exist baseline algorithms. Therefore, we compare our two algorithms with the single-machine variant: SVRGD-P and SVRGD-Z, where SVRGD-P corresponds to DSVRGDA-P and SVRGD-Z corresponds to DSVRGDA-Z. The details of these baseline algorithms can be found in Appendix B. In our experiments, we use 10 workers and the samples are randomly distributed to the workers. Additionally, we use a line graph to connect these workers. For the single-machine baseline algorithms, we also run them on 10 workers but with a fully connected graph. As such, the effective mini-batch size is the same for all algorithms.

<sup>1</sup>We ignore the superscript for simplicity.

<sup>2</sup><https://www.csie.ntu.edu.tw/~cjlin/libsvmtools/datasets/>

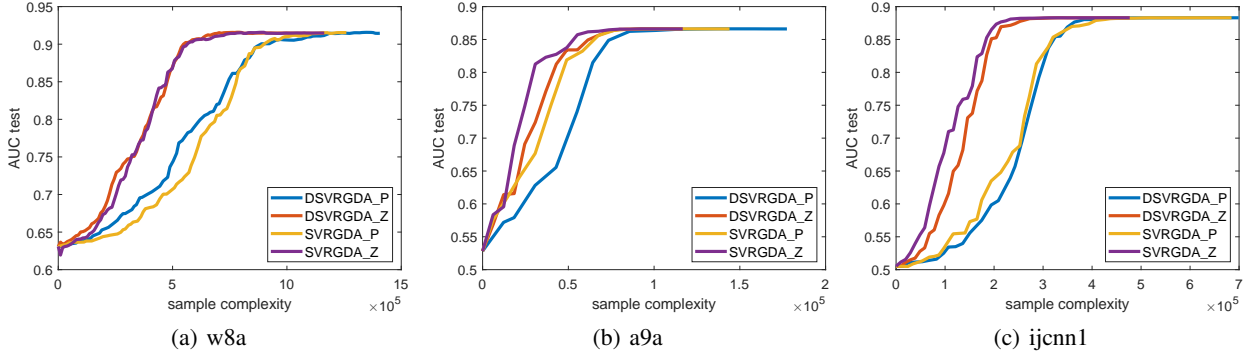


Figure 2: The comparison between different algorithms for Eq. (20). Line graph is used.

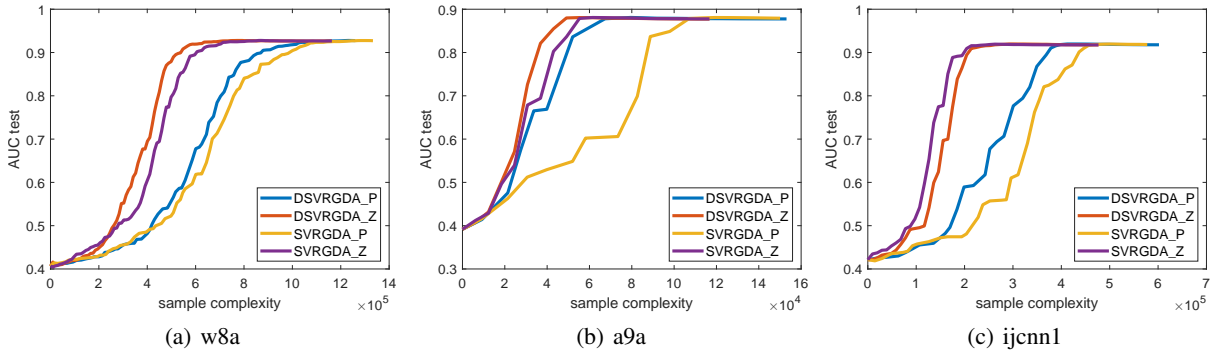


Figure 3: The comparison between different algorithms for Eq. (20). Random graph is used.

In our experiment, the learning rate  $\eta_x$  and  $\eta_y$  are set to 0.01 for all algorithms. As for DSVRGDA-P and SVRGDA-P, the mini-batch size  $b$  is set to  $\sqrt{n}$ , and the probability  $p$  is set to  $b/(n+b)$ . As for DSVRGDA-Z and SVRGDA-Z, the mini-batch size  $b_1$  is also set to  $\sqrt{n}$ , and  $\rho$  is set to  $b_1/(2n)$ . The number of inner iterations  $R$  is set to  $\sqrt{n}$ .

## 6.2 EXPERIMENTAL RESULT

In Figure 1, we show the experimental results on the synthetic data. Specifically, in Figure 1(a), we show  $\|\bar{x} - x^*\|^2 + \|\bar{y} - y^*\|^2$ , which is the distance between the obtained solution from different algorithms to the optimal solution, versus the number of sample complexity. We can observe that our two algorithms demonstrate almost the same convergence behavior as the single-machine counterpart, which confirms the correctness of our algorithms. Moreover, the empirical sample complexity of DSVRGDA-Z is smaller than that of DSVRGDA-P. The reason is that DSVRGDA-Z computes the full gradient only in the initial inner iteration. In Figure 1(b), we plot  $\|[\nabla_x f(x, y)^T, \nabla_y f(x, y)^T]^T\|^2$  versus the sample complexity. The observations are similar to Figure 1(a). Our decentralized algorithms share the similar convergence behavior with the single-machine counterpart and DSVRGDA-Z enjoys a smaller empirical sample complexity. These observations confirm the correctness and effectiveness of our algorithms.

In Figure 2, we show the experimental results on the real-world data. In particular, we show the AUC score of the testing set versus the sample complexity. We can still observe that our decentralized algorithms converge to almost the same value with the single-machine counterparts, which confirms the correctness of our algorithms. Moreover, DSVRGDA-Z enjoys a better empirical sample complexity than DSVRGDA-P.

In Figure 3, the communication graph is an Erdos-Renyi random graph, where the probability for generating edges is 0.5. Under this setting, we have similar observations as the line graph, which further confirms the effectiveness of our algorithms. The results for Eq. (19) can be found in Appendix A.

## 7 CONCLUSION

In this paper, we develop two algorithms for decentralized nonconvex-nonconcave optimization problems that satisfy the PL condition, which demonstrates how to conduct local updates and perform communication to achieve the linear convergence rate. Moreover, our theoretical analyses provide theoretical evidence for our novel algorithmic design. The extensive experimental results confirm the effectiveness of our algorithms.



## References

- Lesi Chen, Boyuan Yao, and Luo Luo. Faster stochastic algorithms for minimax optimization under polyak- $\{L\}$  ojasiewicz condition. In *Advances in Neural Information Processing Systems*, 2022a.
- Lesi Chen, Haishan Ye, and Luo Luo. A simple and efficient stochastic algorithm for decentralized nonconvex-strongly-concave minimax optimization. *arXiv preprint arXiv:2212.02387*, 2022b.
- Ashok Cutkosky and Francesco Orabona. Momentum-based variance reduction in non-convex sgd. *arXiv preprint arXiv:1905.10018*, 2019.
- Cong Fang, Chris Junchi Li, Zhouchen Lin, and Tong Zhang. Spider: Near-optimal non-convex optimization via stochastic path integrated differential estimator. *arXiv preprint arXiv:1807.01695*, 2018.
- Hongchang Gao. Decentralized stochastic gradient descent ascent for finite-sum minimax problems. *arXiv preprint arXiv:2212.02724*, 2022.
- Ian Goodfellow, Jean Pouget-Abadie, Mehdi Mirza, Bing Xu, David Warde-Farley, Sherjil Ozair, Aaron Courville, and Yoshua Bengio. Generative adversarial nets. *Advances in neural information processing systems*, 27, 2014a.
- Ian J Goodfellow, Jonathon Shlens, and Christian Szegedy. Explaining and harnessing adversarial examples. *arXiv preprint arXiv:1412.6572*, 2014b.
- Feihu Huang, Shangqian Gao, Jian Pei, and Heng Huang. Accelerated zeroth-order momentum methods from mini to minimax optimization. *arXiv e-prints*, pages arXiv:2008.2008, 2020.
- Rie Johnson and Tong Zhang. Accelerating stochastic gradient descent using predictive variance reduction. *Advances in neural information processing systems*, 26, 2013.
- Hamed Karimi, Julie Nutini, and Mark Schmidt. Linear convergence of gradient and proximal-gradient methods under the polyak-Łojasiewicz condition. In *Machine Learning and Knowledge Discovery in Databases: European Conference, ECML PKDD 2016, Riva del Garda, Italy, September 19-23, 2016, Proceedings, Part I 16*, pages 795–811. Springer, 2016.
- Zhize Li and Peter Richtárik. Zerosarah: Efficient non-convex finite-sum optimization with zero full gradient computation. *arXiv preprint arXiv:2103.01447*, 2021.
- Zhize Li, Hongyan Bao, Xiangliang Zhang, and Peter Richtárik. Page: A simple and optimal probabilistic gradient estimator for nonconvex optimization. In *International conference on machine learning*, pages 6286–6295. PMLR, 2021.
- Xiangru Lian, Ce Zhang, Huan Zhang, Cho-Jui Hsieh, Wei Zhang, and Ji Liu. Can decentralized algorithms outperform centralized algorithms? a case study for decentralized parallel stochastic gradient descent. In *Advances in Neural Information Processing Systems*, pages 5330–5340, 2017.
- Tianyi Lin, Chi Jin, and Michael Jordan. On gradient descent ascent for nonconvex-concave minimax problems. In *International Conference on Machine Learning*, pages 6083–6093. PMLR, 2020.
- Chaoyue Liu, Libin Zhu, and Mikhail Belkin. Loss landscapes and optimization in over-parameterized non-linear systems and neural networks. *Applied and Computational Harmonic Analysis*, 59:85–116, 2022.
- Mingrui Liu, Zhuoning Yuan, Yiming Ying, and Tianbao Yang. Stochastic auc maximization with deep neural networks. *arXiv preprint arXiv:1908.10831*, 2019.
- Songtao Lu, Xinwei Zhang, Haoran Sun, and Mingyi Hong. Gnsd: a gradient-tracking based nonconvex stochastic algorithm for decentralized optimization. In *2019 IEEE Data Science Workshop, DSW 2019*, pages 315–321. Institute of Electrical and Electronics Engineers Inc., 2019.
- Luo Luo, Haishan Ye, Zhichao Huang, and Tong Zhang. Stochastic recursive gradient descent ascent for stochastic nonconvex-strongly-concave minimax problems. *arXiv preprint arXiv:2001.03724*, 2020.
- Aleksander Madry, Aleksandar Makelov, Ludwig Schmidt, Dimitris Tsipras, and Adrian Vladu. Towards deep learning models resistant to adversarial attacks. *arXiv preprint arXiv:1706.06083*, 2017.
- Lam M Nguyen, Jie Liu, Katya Scheinberg, and Martin Takáč. Sarah: A novel method for machine learning problems using stochastic recursive gradient. In *International Conference on Machine Learning*, pages 2613–2621. PMLR, 2017.
- Maher Nouiehed, Maziar Sanjabi, Tianjian Huang, Jason D Lee, and Meisam Razaviyayn. Solving a class of non-convex min-max games using iterative first order methods. *arXiv preprint arXiv:1902.08297*, 2019.
- Kevin Scaman, Francis Bach, Sébastien Bubeck, Yin Tat Lee, and Laurent Massoulié. Optimal algorithms for smooth and strongly convex distributed optimization in networks. In *international conference on machine learning*, pages 3027–3036. PMLR, 2017.
- Haoran Sun, Songtao Lu, and Mingyi Hong. Improving the sample and communication complexity for decentralized non-convex optimization: Joint gradient estimation and tracking. In *International Conference on Machine Learning*, pages 9217–9228. PMLR, 2020.

Ju Sun, Qing Qu, and John Wright. A geometric analysis of phase retrieval. *Foundations of Computational Mathematics*, 18:1131–1198, 2018.

Thijs Vogels, Lie He, Anastasiia Koloskova, Sai Praneeth Karimireddy, Tao Lin, Sebastian U Stich, and Martin Jaggi. Relaysun for decentralized deep learning on heterogeneous data. *Advances in Neural Information Processing Systems*, 34:28004–28015, 2021.

Wenhan Xian, Feihu Huang, Yanfu Zhang, and Heng Huang. A faster decentralized algorithm for nonconvex minimax problems. *Advances in Neural Information Processing Systems*, 34, 2021.

Ran Xin, Usman A Khan, and Soumya Kar. A near-optimal stochastic gradient method for decentralized non-convex finite-sum optimization. *arXiv preprint arXiv:2008.07428*, 2020.

Junchi Yang, Negar Kiyavash, and Niao He. Global convergence and variance-reduced optimization for a class of nonconvex-nonconcave minimax problems. *arXiv preprint arXiv:2002.09621*, 2020.

Yiming Ying, Longyin Wen, and Siwei Lyu. Stochastic online auc maximization. *Advances in neural information processing systems*, 29:451–459, 2016.

Xin Zhang, Zhuqing Liu, Jia Liu, Zhengyuan Zhu, and Songtao Lu. Taming communication and sample complexities in decentralized policy evaluation for cooperative multi-agent reinforcement learning. *Advances in Neural Information Processing Systems*, 34:18825–18838, 2021.